

Analytical model to evaluate interface characteristics of carbon nanotube reinforced aluminum oxide nanocomposites

Yao Chen, Kantesh Balani, and Arvind Agarwal^{a)}

Mechanical and Materials Engineering Department, EC 3464, Florida International University, 10555 West Flagler Street, Miami, Florida 33174, USA

(Received 5 October 2007; accepted 13 November 2007; published online 7 January 2008)

This research presents an analytical method to investigate the effect of volume fraction and the number of outer walls of multiwalled carbon nanotube (MWNT) reinforcement on load carrying capability in the aluminum oxide matrix. Interfacial shear stress transfer and energy dissipation have been estimated using the Cox model. Critical energy release rate for the debonding of MWNT from the matrix is also estimated based on the crack deflection. The computed results sufficiently manifest that MWNT pullout and crack deflection contributes greatly to improved fracture toughness of carbon nanotube reinforced aluminum oxide nanocomposites. © 2008 American Institute of Physics. [DOI: 10.1063/1.2821108]

One of the applications of carbon nanotubes (CNTs) is as ultrastrong reinforcement for nanocomposite materials.^{1,2} Recent research^{3–6} reveals that CNTs are promising toughening agents for brittle ceramic matrices. Zhan *et al.*³ fabricated CNT/aluminum oxide nanocomposite by blending dispersed single-walled CNTs with nanocrystalline aluminum oxide powders followed by the spark plasma sintering. Fracture toughness of the CNT reinforced aluminum oxide was three times that of unreinforced aluminum oxide.³ Fan *et al.*⁴ reported 100% improvement in the fracture toughness of single-wall carbon nanotube reinforced aluminum oxide, which was attributed to the strong interface between CNTs and the matrix obtained by heterocoagulation. It is well known that interfacial shear stress is a critical parameter controlling the efficiency of stress transfer from the matrix to the fiber and, hence, affecting overall mechanical properties such as elastic modulus and tensile strength.⁵ Hence, in-depth understanding of the reinforcing and toughening mechanisms of CNTs demands evaluation of the shear stress at CNT/matrix interface. Much of the research on the interfacial shear stress in CNT reinforced composites is limited to polymer matrix nanocomposites.^{5–8} Wagner *et al.*⁶ estimated the interfacial shear stress of 500 MPa for multiwalled carbon nanotubes (MWNT)/polyurethane thin film. Barber *et al.*⁷ measured the interfacial shear stress (20–90 MPa) between MWNT and the polyethylene matrix by mounting a multiwalled CNT onto the atomic force microscope tip and, subsequently, pushing it into heated polymer film and then pulling the tube out from the cured polymer. Molecular dynamics simulation has been employed to evaluate interfacial shear stress of 160 MPa for CNT/polystyrene⁸ and 138 MPa for CNT/epoxy composite.⁵ In our previously published research,^{9,10} Al₂O₃ nanocomposite coatings with addition of 6.20 and 12.47 vol. % MWNTs were synthesized using plasma spraying. Al₂O₃-MWNT nanocomposite coating displayed an improvement in the fracture toughness of up to 57% (3.22, 4.60, and 5.04 MPa m^{1/2}, respectively, for Al₂O₃ with 0.0, 6.20, and 12.47 vol. % CNT reinforcement).^{9,11} The aim of the present research is to compute interfacial shear

stress and energy dissipated by MWNT pullout and crack deflection in the Al₂O₃ ceramic matrix using an analytical model. It will assist in better understanding of the toughening mechanisms in CNT/ceramic nanocomposites, which are sparsely investigated in comparison to CNT/polymer nanocomposites. The details of the processing and microstructure can be found elsewhere.⁹

Carbon atoms within each rolled graphite layer in MWNT have strong covalent bonding. However, bonding between concentric graphite layers is weak, arising from the van der Waals interaction.¹² The weak bonding between the concentric layers results in the decrease in load transfer.¹² As a result, it is hypothesized that the outer wall layers of the MWNTs carry the maximum load transferred at the MWNT/matrix interface.¹² Figure 1(a) shows the schematic illustration of cross section of MWNT, in which h (~ 0.75 Å)¹³ is the effective layer (wall) thickness, d (~ 3.4 Å)¹³ is the spacing between each grapheme layer, R_{CNT} is the radius of the MWNT, and ρ_0 is the radius of the first inner layer of MWNT. The area of outer wall layers carrying load can be computed using

$$A_{\text{eff}} = \pi \sum_{m=1}^N \{ [R_{\text{CNT}} - (m-1)h - (m-1)h']^2 - [R_{\text{CNT}} - mh - (m-1)h']^2 \}, \quad (1)$$

where $h' = d - h$, and N is the number of outer layers carrying load.

The Cox model,^{14–16} assuming perfect interface bonding, is employed to analyze the interfacial shear stress between

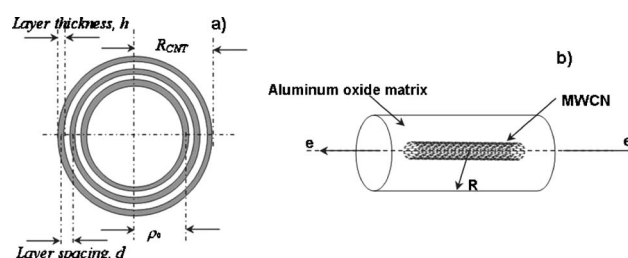


FIG. 1. Schematic illustration of (a) cross section of MWNT and (b) single MWNT/aluminum oxide composite cylinder under applied strain.

^{a)} Author to whom corresponding should be addressed. Tel.: 305-348-1701. Fax: 305-348-1932. Electronic mail: agarwala@fiu.edu.

the CNTs and the aluminum oxide matrix. Fig. 1(b) shows a schematic illustration of MWNT with radius R_{CNT} and length L , located at the center of a coaxial cylindrical aluminum oxide matrix with radius R . The Cox model presents the following equations to simulate interfacial shear stress along the longitudinal axis of MWNT:

$$\tau = \frac{E_{\text{CNT}} \times e \times A_{\text{eff}} \times \beta}{2\pi R_{\text{CNT}}} \times \frac{\sinh \beta(L/2 - x)}{\cosh \beta L/2}, \quad (2)$$

$$\beta = \sqrt{\left(\frac{G'_{\text{Al}_2\text{O}_3}}{E_{\text{CNT}}}\right) \left(\frac{2\pi}{A_{\text{eff}} \ln R/R_{\text{CNT}}}\right)}, \quad (3)$$

where τ is the interfacial shear stress along the longitudinal axis of MWCNT, E_{CNT} is the elastic modulus of MWNT, A_{eff} is the effective area of the outer wall layers carrying load, $G'_{\text{Al}_2\text{O}_3}$ is the shear modulus of aluminum oxide, e is the applied strain, and x is the distance from the ends of the MWNT.

The volume fractions of MWNTs for 4 wt. % CNT aluminum oxide and 8 wt. % CNT aluminum oxide nanocomposite were estimated to be 6.20% and 12.47%, respectively.¹⁰ Also, the diameter of employed MWNTs in this research varies in the range of 40–70 nm. The radius of the single MWNT composite cylinder can be related to the MWNT volume fraction based on following equation:¹⁶

$$\left(\frac{R}{R_{\text{CNT}}}\right)^2 = \frac{\pi}{4V_f}. \quad (4)$$

Therefore, the ratio of R/R_{CNT} is simulated to be 3.56 for 6.20 vol. % MWNT aluminum oxide composite, and 2.51 for 12.47 vol. % MWNT aluminum oxide composite.

In the following computations, $G'_{\text{Al}_2\text{O}_3}=152$ GPa,¹⁷ $E_{\text{CNT}}=800$ GPa, and $e=1\%$ ¹⁶ are employed. Also, two different radii of MWNTs with $R_{\text{CNT}}=35$ nm and $R_{\text{CNT}}=20$ nm are used in the computations to obtain the upper and the lower limits of the effect of MWNT geometry on their interfacial behavior. The shear stress exhibits its maximum value at the two ends of the nanotube/fiber.¹⁶ The maximum values of the interfacial shear stress are taken into account for the computation. The relationship between maximum interfacial shear stress and outer layer numbers of MWNT carrying load are shown in Fig. 2(a). It is evident that the maximum value of the interfacial shear stress increases with the number of outer layer of MWNT carrying load.

It is a well known that the fiber-matrix interface fails when debonding occurs under larger interfacial shear stress followed by the fiber pullout. The energy dissipation by the fiber pullout contributes largely to the improvement in the fracture toughness of the fiber reinforced composites. Similarly, for MWNT reinforced Al_2O_3 nanocomposites, the energy dissipation by MWNT pullout is also expected to be the main toughening mechanism. Based on the experimental observations,⁹ MWNT pullout length in the plasma sprayed Al_2O_3 ranges from ~ 100 to 300 nm. The energy dissipation by the MWNT pullout can be expressed by the following equation:¹⁸

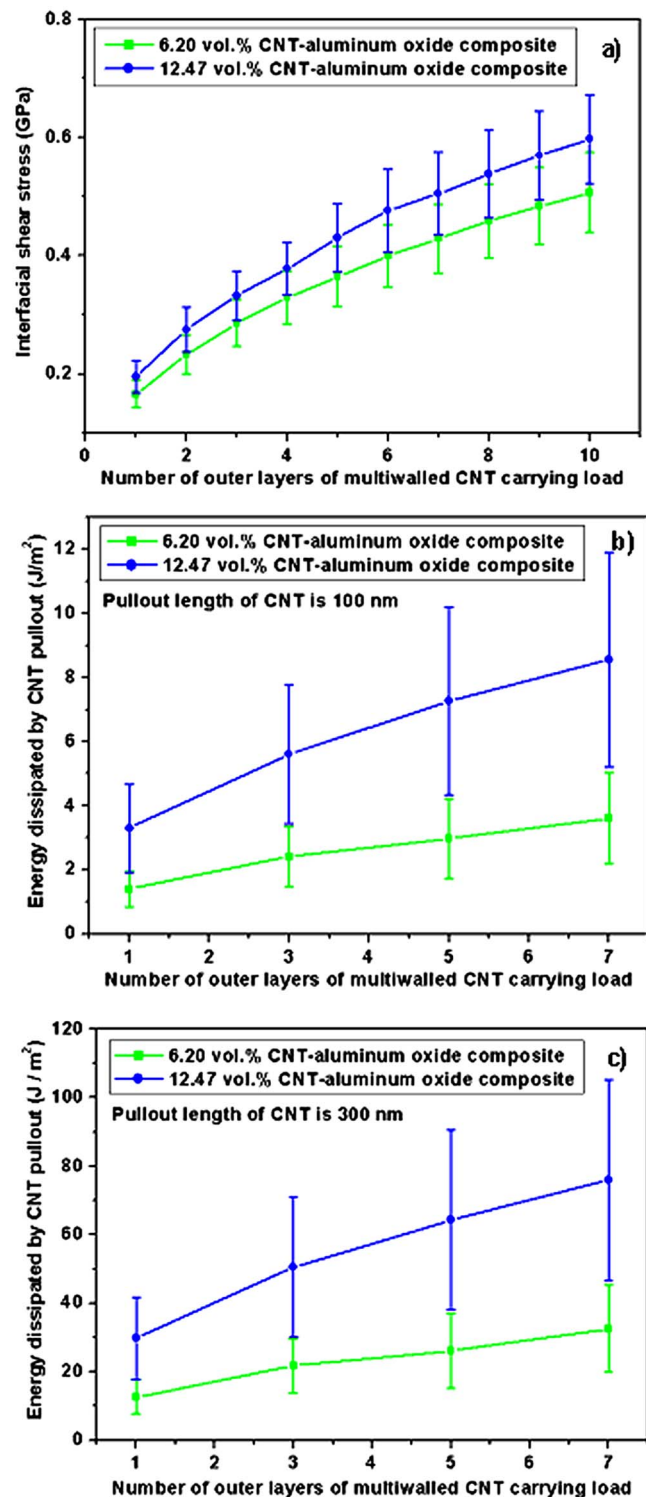


FIG. 2. (Color online) (a) Relationship of maximum value of interfacial shear stress between the numbers of outer layers of MWNT carrying load. Computed energy dissipated by MWNT pullout with the variation of outer layers carrying load for pullout length of (b) 100 nm and (c) 300 nm. Error bars correspond to the upper and lower limits of assumptions used in the calculation for MWNT geometry.

$$G_{\text{pullout}} = \frac{V_f l^2 \tau}{3R_{\text{CNT}}}, \quad (5)$$

where V_f is the volume fraction of MWNTs, τ is the maximum value of interfacial shear stress, l is the pullout length of MWNTs, and R_{CNT} is the radius of MWNTs. Hence, the dissipated energy by the MWNT pullout is computed by

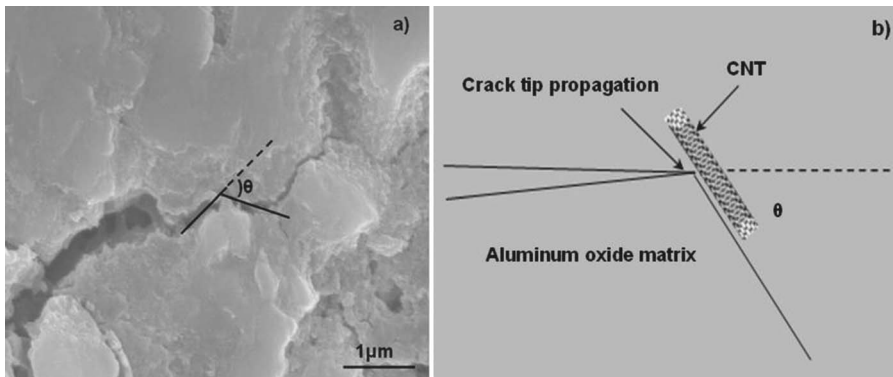


FIG. 3. (a) Scanning electron microscopy (SEM) image showing crack deflection in MWNT aluminum oxide composite and (b) schematic illustration of crack deflection when crack tip reaches MWNT.

varying the number of load carrying outer layers for pullout length of MWNT as 100 and 300 nm, respectively [Figs. 2(b) and 2(c)]. The computed results indicate that the energy dissipated by the MWNT pullout increases with the number of outer layers carrying load for a constant volume fraction of MWNTs. It implies that increase in the number of outer layers of MWNT carrying load contributes to its toughening effect. Figure 2(c) shows that energy dissipation increases for a longer length (300 nm) of MWNT pullout due to creation of the larger surface area.

In addition to the MWNT pullout mechanism, crack deflection by nanotubes is also regarded as another toughening mechanism.^{9,19} Figure 3(a) shows a crack initiated from the tip of indent and subsequent crack deflection in MWNT reinforced aluminum oxide composite. Assuming, the crack tip reach the MWNT and then deflects to another direction (along MWNT matrix interface). The angle between the two directions is θ [Fig. 3(b)]. The critical energy release rate for the debonding of the MWNT/ceramic interface is denoted G_C^{CNT} whereas the energy release rate for the crack advancing along its original direction is G_A and G_B for the crack advancing along MWNT/ceramic interface. They must follow the relationship²⁰

$$G_B = G_A \cos^4(\theta/2). \quad (6)$$

Based on the deflection criterion, the crack deflection can occur if

$$\frac{G_A}{G^{\text{Al}_2\text{O}_3}} > \frac{G_B}{G_C^{\text{CNT}}}, \quad (7)$$

where $G^{\text{Al}_2\text{O}_3}$ is the fracture energy of aluminum oxide and, therefore,

$$G_C^{\text{CNT}} > G^{\text{Al}_2\text{O}_3} \cos^4(\theta/2). \quad (8)$$

It is known that the fracture energy of aluminum oxide is approximately 33.83 Jm^{-2} .²⁰ As seen from Fig. 3(a), the crack deflection angle is $\sim 60^\circ$. From Eq. (6) and (8) and crack deflection of 60° , it is concluded that the critical energy release rate, G_C^{CNT} for the debonding of MWNT is greater than 19.03 Jm^{-2} . The critical energy release rate for the debonding of MWNT (19.03 Jm^{-2}) is lower than the fracture energy of aluminum oxide (33.83 Jm^{-2}). Consequently, MWNT matrix debonding occurs first and dissipates energy by the creation of new surfaces. Uniform MWNT

dispersion and high surface area associated with the nanotubes impart uniform sites for energy release.¹¹ Increased fracture toughness of up to 57% has been observed for MWNT reinforced aluminum oxide composite,^{10,11} which is attributed to energy dissemination (by interfacial shear) at the MWNT matrix interface.

In summary, the interfacial shear stress transfer behavior and the energy dissipation by MWNT pullout are investigated using Cox model, in which the volume fraction of MWNT and numbers of outer wall layer of MWNT carrying load are taken into account. Additionally, critical energy release rate for the debonding of MWNT is also estimated based on the crack deflection. The results sufficiently indicate that increase in the number of outer layers of MWNT carrying load contributes to the improved fracture toughness.

The authors acknowledge the financial support received from the Office of Naval Research (N00014-05-1-0398) and National Science Foundation-CAREER (DMI 0547178).

¹P. G. Collins and Ph. Avouris, *Sci. Am.* **283**, 38 (2000).

²W. A. Curtin and B. W. Sheldon, *Mater. Today* **7**, 44 (2004).

³G. D. Zhan, J. D. Kuntz, J. L. Wan, and A. K. Mukherjee, *Nat. Mater.* **2**, 38 (2003).

⁴J. P. Fan, D. W. Zhuang, D. Q. Zhao, G. Zhong, and M. S. Wu, *Appl. Phys. Lett.* **89**, 121910 (2006).

⁵M. Wong, M. Paramsothy, X. J. Xu, Y. Ren, S. Li, and K. Liao, *Polymer* **44**, 7757 (2003).

⁶H. D. Wagner, O. Lourie, Y. Feldman, and R. Tenne, *Appl. Phys. Lett.* **72**, 188 (1998).

⁷A. H. Barber, S. R. Cohen, S. Kenig, and H. D. Wagner, *Compos. Sci. Technol.* **64**, 2283 (2004).

⁸K. Liao and S. Li, *Appl. Phys. Lett.* **79**, 4225 (2001).

⁹K. Balani, S. B. Rao, Y. Chen, T. Laha, and A. Agarwal, *J. Nanosci. Nanotechnol.* **7**, 3553 (2007).

¹⁰Y. Chen, K. Balani, and A. Agarwal, *Appl. Phys. Lett.* **91**, 031903 (2007).

¹¹K. Balani, Ph.D. thesis, Florida International University, 2007.

¹²E. T. Thostenso and T. W. Chou, *J. Phys. D* **36**, 573 (2003).

¹³K. T. Lau, *Chem. Phys. Lett.* **370**, 399 (2003).

¹⁴H. L. Cox, *Br. J. Appl. Phys.* **3**, 72 (1952).

¹⁵A. Kelly and N. H. Macmillan, *Strong Solids*, 3rd ed. (Clarendon, Oxford, 1986), p. 240.

¹⁶K. Q. Xiao and L. C. Zhang, *J. Mater. Sci.* **39**, 4481 (2004).

¹⁷C. A. Happer, *Handbook of Ceramics, Glasses and Diamonds*, 1st ed. (McGraw-Hill, New York, 2001), p. 433.

¹⁸B. Fiedler, F. H. Gojney, M. H. G. Wichmann, M. C. M. Nolte, and K. Schuler, *Compos. Sci. Technol.* **66**, 3115 (2006).

¹⁹Z. Xia, L. Riester, W. A. Curtin, H. Li, B. W. Sheldon, J. Liang, B. Chang, and J. M. Xu, *Acta Mater.* **52**, 931 (2004).

²⁰H. L. Tan and W. Yang, *Mech. Mater.* **30**, 111 (1998).